Electronic Supplementary Material (ESI) for Analytical Methods.
This journal is © The Royal Society of Chemistry 2024

Hemicyanine-based near-infrared fluorescent probe with large Stokes shift for non-invasive bioimaging of brown adipose tissue

Ke Xiang,[a] Jinbin Pan,[b] Jiaojiao Yu,[a] Lehui Xiao,[c] Shao-Kai Sun*[a] and Ran Cheng*[a]

a. School of Medical Imaging, Tianjin Key Laboratory of Functional Imaging, Tianjin Medical University, Tianjin 300203, China.

b. Department of Radiology, Tianjin Key Laboratory of Functional Imaging, Tianjin Medical University General Hospital, Tianjin, 300052, China.

c. College of Chemistry and Chemical Engineering, Central South University, Changsha 410083, China

**E-mail*: shaokaisun@tmu.edu.cn; rancheng@tmu.edu.cn

Table of Contents

1. Synthetic procedures

Synthesis of 5-(4-(dimethylamino)phenyl)thiophene-2-carbaldehyde (**3a**).

Aldehyde **3a** was prepared according to the previous reported method with minor modifications.[1] (4-(dimethylamino)phenyl)boronic acid **1a** (330 mg, 2 mmol) and 5-bromothiophene-2-carbaldehyde **2** (382 mg, 2 mmol) were dissolved in a mixture of dioxane (5 mL), aqueous K_2CO_3 (2 mL, 4 M) and ethanol (2 mL). And then [$Pd(PPh_3)_4$] (69 mg, 0.06 mmol) was added immediately. The mixture was heated to 85 °C and stirred for 4 h under Ar atmosphere. After the reaction was completed, the mixture was cooled down to room temperature. Water (30 mL) was added to quench the reaction and the mixture was extracted with ethyl acetate (3 × 30 mL). The combined organic layers were dried by anhydrous Na_2SO_4. After filtered and evaporated, the residue was purified by silica gel chromatography with eluent of petroleum ether/ethyl acetate (v/v = 4:1) to afford a yellow solid. Yield: 88%. Melting point: 245-248 ^oC. ^1H NMR (400 MHz, $CDCl_3$) δ 9.82 (s, 1H), 7.68 (d, J = 4.0 Hz, 1H), 7.56 (d, J = 8.8 Hz, 2H), 7.24 (d, J = 4.0 Hz, 1H), 6.73 (d, J = 8.4 Hz, 2H), 3.02 (s, 6H); ^{13}C NMR (100 MHz, $CDCl_3$) δ 182.43, 155.99, 151.07, 140.12, 138.10, 127.52, 121.57, 120.92, 112.20, 40.27.

Synthesis of 5-(4-(diphenylamino)phenyl)thiophene-2-carbaldehyde (**3b**).

The reaction was carried out according to the procedure used for the synthesis of **3a** by using **1b** as starting material. Yellow solid. Yield: 82%. Melting point: 218-220 ^oC. ^1H NMR (400 MHz, DMSO-d_6) δ 9.87 (s, 1H), 8.00 (d, J = 4.0 Hz, 1H), 7.70 (d, J = 8.8 Hz, 2H), 7.61 (d, J = 4.0 Hz, 1H), 7.47 – 7.26 (m, 4H), 7.21 – 7.06 (m, 6H), 6.97 (d, J = 8.7 Hz, 2H); ^{13}C NMR (100 MHz, $CDCl_3$) δ 182.63, 154.60, 149.15, 146.97, 141.30, 137.80, 129.50, 127.28, 126.12, 125.18, 123.89, 122.91, 122.39.

Synthesis of 4-(1,1,2-trimethyl-1*H*-benzo[*e*]indol-3-ium-3-yl)butane-1-sulfonate (**5a**).

Compound **5a** was prepared according to the previous reported method with minor modifications.[2] 1,4-Butylenesulfone (3.07 mL, 30 mmol) and 1,1,2-trimethyl-1*H*-benzo[*e*]indole **4** (2.09 g, 10 mmol) were added into a 100 mL round bottom flask. The

mixture was heated to 135 °C and stirred for 2 h under Ar atmosphere. After cooling down to room temperature, ethyl acetate was added and the mixture was treated by ultrasound to produce precipitation. The obtained precipitation was filtered and washed with ethyl acetate. The target compound was achieved as light blue solid. Yield: 89%. Melting point: 161-164 °C. ^{1}H NMR (400 MHz, DMSO-d_6) δ 8.36 (d, J = 8.3 Hz, 1H), 8.28 (d, J = 8.9 Hz, 1H), 8.24 – 8.19 (d, J = 8.9 Hz, 2H), 7.78 (t, J = 7.1 Hz, 1H), 7.72 (t, J = 7.3 Hz, 1H), 4.61 (t, J = 7.8 Hz, 2H), 2.95 (s, 3H), 2.56 – 2.50 (m, 2H), 2.04 (p, J = 7.4 Hz, 2H), 1.84 – 1.72 (m, 8H); ^{13}C NMR (100 MHz, DMSO-d_6) δ 196.82, 139.09, 137.35, 133.48, 131.12, 130.18, 128.80, 128.74, 127.66, 123.85, 113.94, 55.91, 50.60, 47.98, 26.69, 22.61, 22.05, 14.14.

Synthesis of 3-ethyl-1,1,2-trimethyl-1*H*-benzo[*e*]indol-3-ium iodide (**5b**).

5b was prepared according to the previous reported method with minor modifications.[3] Iodoethane (880 μL, 11 mmol) was added dropwise to a mixture of **4** (2.09 g, 10 mmol) in *o*-dichlorobenzene (8 mL), then the reaction was heated to 110 °C and stirred for 6 h under Ar atmosphere. After cooling down to room temperature, ethyl acetate was added and the mixture was treated by ultrasound to produce precipitation. The obtained precipitation was filtered and washed with ethyl acetate. The target compound was achieved as gray solid. Yield: 65%. Melting point: 110-113 °C. ^{1}H NMR (400 MHz, DMSO-d_6) δ 8.39 (d, J = 8.3 Hz, 1H), 8.32 (d, J = 8.9 Hz, 1H), 8.24 (d, J = 8.1 Hz, 1H), 8.19 (d, J = 8.9 Hz, 1H), 7.81 (t, J = 7.2 Hz, 1H), 7.74 (t, J = 7.3 Hz, 1H), 4.65 (q, J = 7.3 Hz, 2H), 2.98 (s, 3H), 1.78 (s, 6H), 1.53 (t, J = 7.3 Hz, 3H); ^{13}C NMR (100 MHz, DMSO-d_6) δ 196.39, 138.65, 137.48, 133.48, 131.17, 130.18, 128.87, 127.72, 127.70, 123.88, 113.68, 55.93, 43.87, 21.97, 14.28, 13.40.

2. Quantum yield

The quantum yield was measured according to the previous reported procedure using indocyanine green (ICG) as a reference ($\Phi_{F(S)}$ = 0.13 in DMSO).[4] Probes were dissolved in dichloromethane or normal saline (NS), The quantum yield was calculated using the following equation:

$$\Phi_{F(X)} = \Phi_{F(S)} (A_S F_X / A_X F_S) (\eta_X / \eta_S)^2$$

Where $\Phi_{F(X)}$ is the fluorescence quantum yield of the probe, A_X and A_S are the absorbance of **HCYBAT-1-3** (**HCYBATs**) and ICG at 650 nm (≤ 0.05), respectively. The area under the curve (AUC) of ICG and **HCYBATs** from 700-900 nm with 650 nm excitation was calculated as F_S and F_X, and η is the refractive index of the solvents.

3. pH stability assessment

10 μM stock solution of the three probes were dissolved in buffer solution, fluorescence intensity was recorded in a wide pH range (4.0-10.0).

4. Photostability assessment

10 μM probe DMSO solutions were irradiated by a 60 W iodine-tungsten lamp. Fluorescence intensity was recorded at different time points. The fluorescence intensity at 0 h was set as a reference (F_0).

5. Colloidal stability assessment

HCYBATs (10 μM) were incubated at 37 °C with water, saline, and fetal bovine serum (FBS) for 2 h and photographed at different time points.

6. The measurement of lipophilicity (Log*P*)

Lipophilicity was evaluated as Log*P* value, which was performed according to the reported flask shaking method.[5] Probes (20 μL, 1 mM in DMSO) were partitioned in a mixture of *n*-octanol (0.99 mL) and NS (0.99 mL) in a test tube. After vortexing at 2000 rpm for 5 min, the tube was centrifuged at 6000 rpm for 5 min. After the octanol layer was separated from the water layer, 10 μL aliquot of each layer was injected into a Waters E2695 HPLC and the absorbance was measured. The Log*P* was defined as Log [ratio between the amount of test compound in octanol and water solution]. The procedure was repeated at least triplicate.

7. Cell culture and cytotoxicity assay

3T3, 4T1 and HepG2 cells were cultured in Dulbecco's Modified Eagle Medium (DMEM, Hyclone) supplemented with 1% penicillin and streptomycin and 10% FBS (Hyclone). Methyl thiazolyl tetrazolium (MTT) assays were performed to assess the cytotoxicity of **HCYBATs** on different cells. Tested cells were seeded into 96-well plates with total volumes of 200 μL per well at a density of 10^4 and incubated at 37 °C in 5% CO_2 for 24 h. After that, unfresh medium was abandoned, then various concentrations of **HCYBATs** were added (0, 5, 10, 20, 30, 40, 50, 100 μM). 24 h later, each well was replaced with fresh medium containing 10 μL of MTT solution (5 mg/mL) and incubated for another 4 h. The medium was continued to be incubated for 4 h. After that, the medium was carefully removed, and 120 μL of DMSO was added in each well to disperse the formazan. Finally, the absorbance at 490 nm was measured by microplate reader (Bio-Tek, USA).

8. Monitoring BAT activation

In this work, BAT activation was induced in normal C57BL/6 mice by norepinephrine (NE) administration or cold exposure. Firstly, NE (0.4 mg/kg) was intravenously injected via tail vein 5 min before the intravenous injection of **HCYBAT-1** (5.4 μmol/kg). While same volume of saline was administrated instead of NE in the normal group. Images were taken at different time points (2 min, 5 min, 10 min, 15 min, 20 min, 30 min, 40 min, 50 min and 60 min) after probe injection. To confirm the *in vivo* imaging results, BAT and WAT were harvested at 10 minutes postinjection. *In vivo* and *ex vivo* imaging was performed under same imaging conditions as mentioned above.

Monitoring BAT activation under cold exposure with **HCYBAT-1**: The experimental group of C57BL/6 mice was placed in 4 °C environment for 12 h before intravenous injection of **HCYBAT-1**. While normal group was placed at room temperature (25 °C). Images were taken at different time points (2 min, 5 min, 10 min,

15min, 20 min, 30 min, 40 min, 50 min and 60 min) after injection of the probe. To confirm the *in vivo* imaging results, BAT and WAT were harvested at 10 minutes postinjection. *In vivo* and *ex vivo* imaging was performed under same imaging conditions as mentioned above.

9. Biocompatibility assessment

The *in vivo* biocompatibility of **HCYBAT-1** was evaluated by body weight recording, blood biochemical examination and histopathology. **HCYBAT-1** (5.4 μmol/kg, n = 5) was injected intravenously in mice as experimental group, while same amount of saline (n = 5) was used for the mice in control group. The weights were recorded every day during 14 days. Then, serum was collected from mice of control, 1 day, 7 days and 14 days postinjection group, respectively, to analyze blood biochemical indicators including alanine aminotransferase (ALT), aspartate aminotransferase (AST), alkaline phosphatase (ALP), total protein (TP), serum albumin (ALB), serum creatinine (CREA), uric acid (UA) and blood urea (UREA).

Wild-type mice were injected with **HCYBAT-1** (5.4 μmol/kg) via tail vein and were sacrificed at 1, 7, and 14 days postinjection, while control group received same amount of saline via intravenous injection (n = 5 at each time point). Major organs including liver, lungs, kidneys, spleen and heart were collected, fixed with 4% paraformaldehyde, and stained with hematoxylin & eosin (H&E).

10. Table S1. Photophysical properties and lipophilicity of **HCYBATs**

Probe	λ_{abs} (nm)	λ_{ex} (nm)	λ_{em} (nm)	Stokes shift (nm)	ε (M^{-1} cm^{-1})	Φ(%) (NS/DCM)	Log*P*
HCYBAT-1	648.5	642	781	139	46970	0.5/15	2.234
HCYBAT-2	676.5	646	777	131	54460	0.4/7	3.354
HCYBAT-3	620.5	610	836	226	65440	0.8/2	1.351

11. Supplemental figures

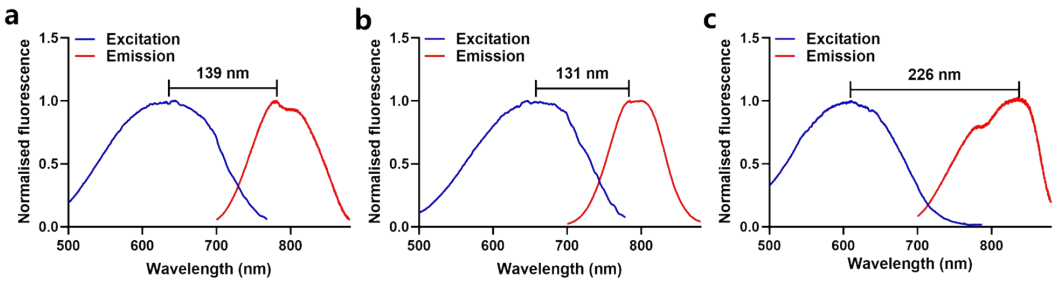

Fig. S1 Normalized excitation and emission spectra of **HCYBAT-1** (a), **HCYBAT-2** (b) and **HCYBAT-3** (c) in DCM.

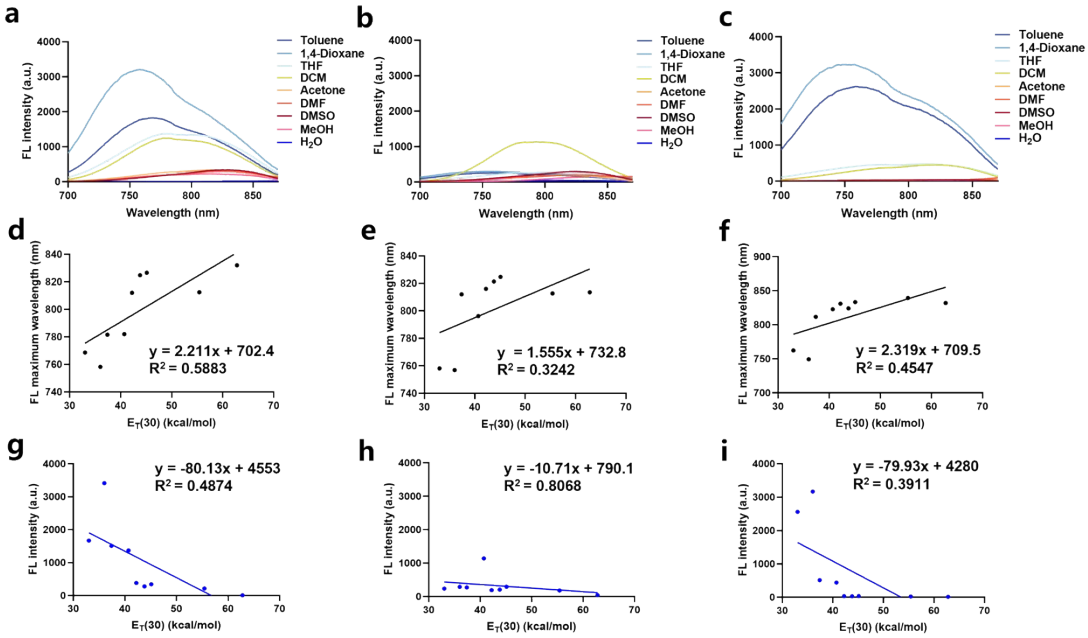

Fig. S2 Polarity response measurements. Fluorescence spectra of **HCYBAT-1** (a), **HCYBAT-2** (b) and **HCYBAT-3** (c) in solvents with different polarity (toluene ($E_T(30)$ = 33.0), 1,4-dioxane ($E_T(30)$ = 36.0), THF ($E_T(30)$ = 37.4), DCM ($E_T(30)$ = 40.7), acetone ($E_T(30)$ = 42.2), DMF ($E_T(30)$ = 43.8), DMSO ($E_T(30)$ = 45.1), methanol ($E_T(30)$ = 55.4) and water ($E_T(30)$ = 62.8). Linearity between maximum emission wavelength of **HCYBAT-1** (d), **HCYBAT-2** (e) and **HCYBAT-3** (f) and $E_T(30)$. Linearity between fluorescence intensity of **HCYBAT-1** (g), **HCYBAT-2** (h) and **HCYBAT-3** (i) and $E_T(30)$. 10 μM, λ_{ex} = 597 nm.

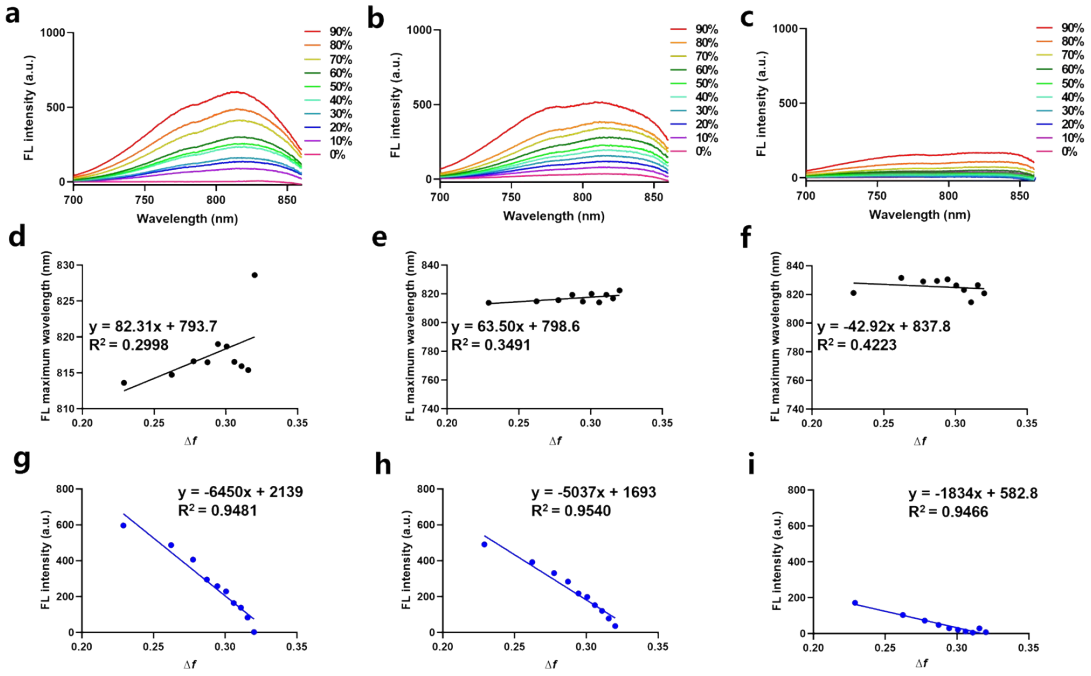

Fig. S3 Polarity response measurements. Fluorescence spectra of **HCYBAT-1** (a), **HCYBAT-2** (b) and **HCYBAT-3** (c) in mixtures of 1,4-dioxane and water, with 1,4-dioxane from 0 to 90%. Linearity between maximum emission wavelength of **HCYBAT-1** (d), **HCYBAT-2** (e) and **HCYBAT-3** (f) and Δ*f*. Linear response between fluorescence intensity of **HCYBAT-1** (g), **HCYBAT-2** (h) and **HCYBAT-3** (i) and Δ*f*. 10 μM, λ_{ex} = 597 nm.

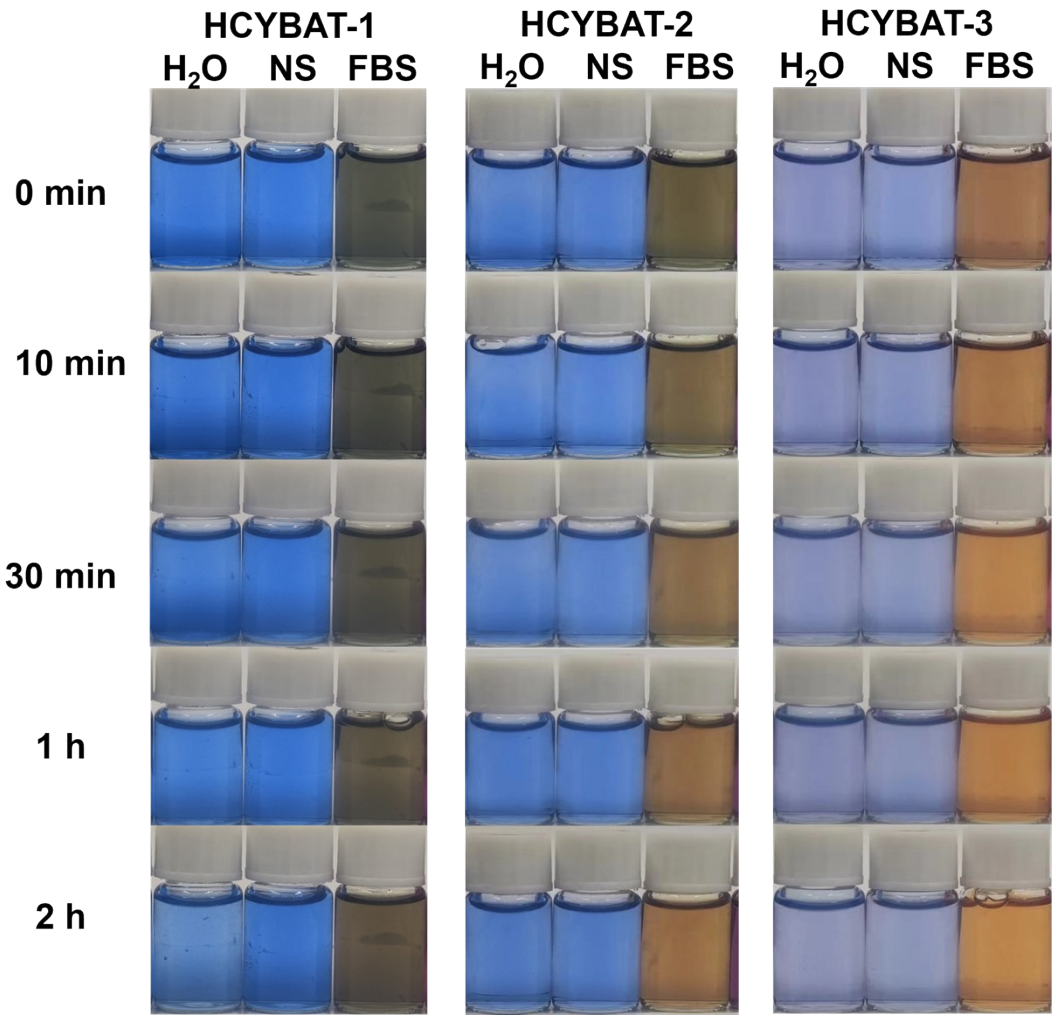

Fig. S4 The photographs of **HCYBATs** dissolved in different media including H_2O, normal saline and FBS.

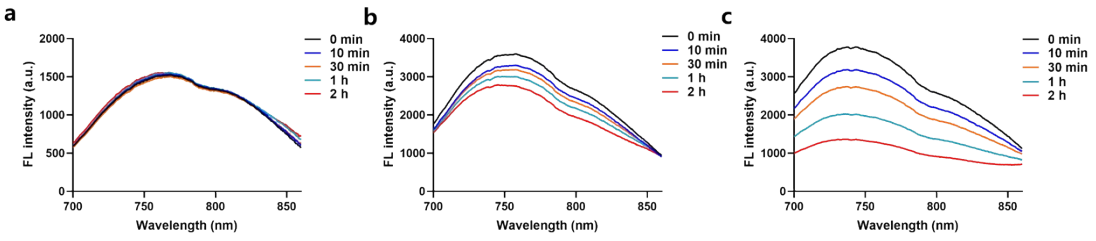

Fig. S5 Fluorescence spectra of **HCYBAT-1** (a), **HCYBAT-2** (b) and **HCYBAT-3** (c) in FBS at different time points.

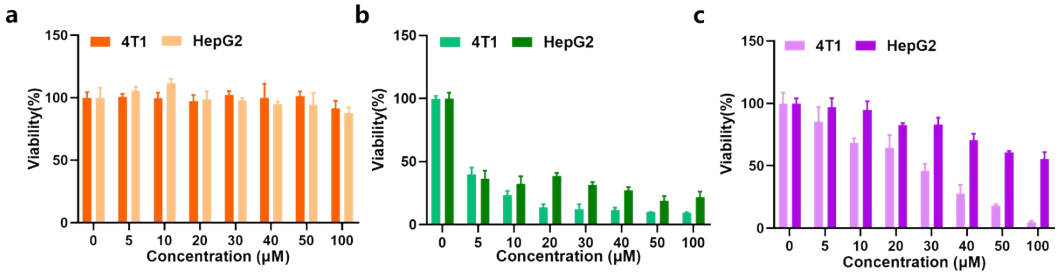

Fig. S6 (a) Cytotoxicity of **HCYBAT-1** to 4T1 and HepG2 cell lines. (b) Cytotoxicity of **HCYBAT-2** to 4T1 and HepG2 cell lines. (c) Cytotoxicity of **HCYBAT-3** to 4T1 and HepG2 cell lines.

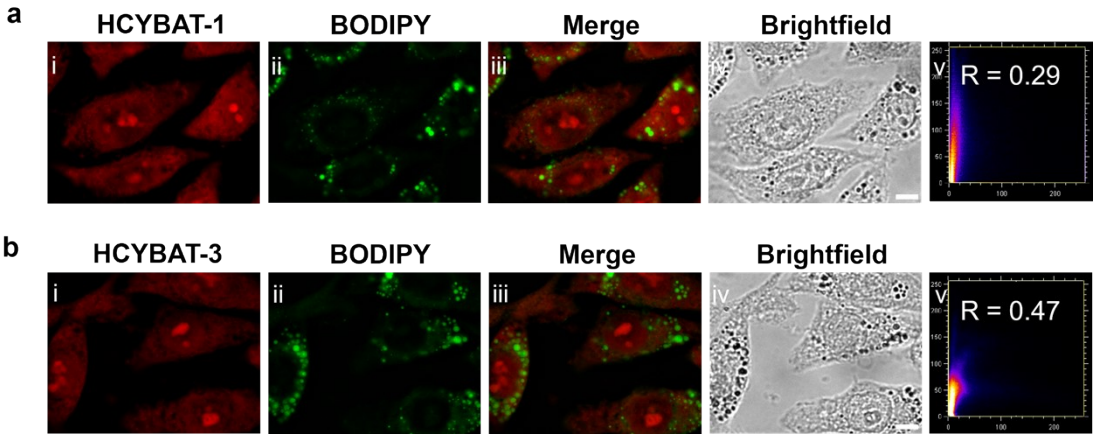

Fig. S7 Colocalization experiment in HepG2 cells. The HepG2 cells were incubated with BODIPY (100 nM) for 1 h and (a) **HCYBAT-1** or (b) **HCYBAT-3** (20 μM) for 30 min. (i) Fluorescence image of probe in the red channel (λ_{ex} = 635 nm, λ_{em} = 700 nm). (ii) Microscopic image of BODIPY in the green channel (λ_{ex} = 475 nm, λ_{em} = 510 nm). (iii) Merged image of the green and the red channels. (iv) Brightfield image. (v) Pearson's correlation coefficient of probe and tracker. Scale bar: 5 μm.

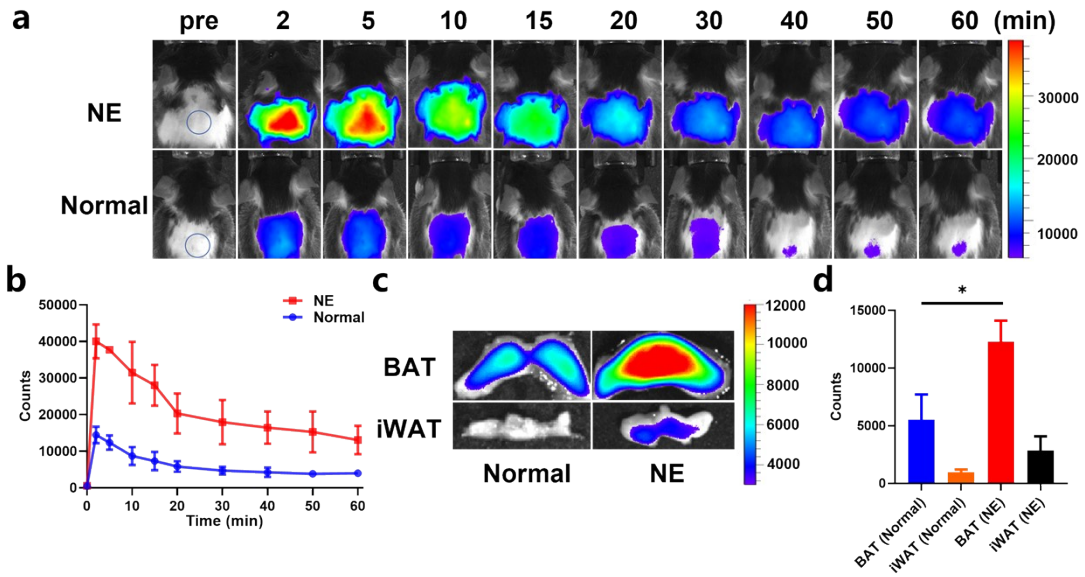

Fig. S8 Evaluation of **HCYBAT-1** for monitoring BAT activation in response to norepinephrine (NE) treatment. (a) Fluorescence images of norepinephrine-treated (NE) and control mice (Normal) (n = 3) at different time points (λ_{ex} = 710 nm, λ_{em} = 810 - 875 nm). (b) Fluorescent signals of NE and Normal group at different time points (λ_{ex} = 710 nm, λ_{em} = 810-875 nm). *Ex vivo* fluorescence images (c) and intensity analysis (d) of interscapular WAT (iWAT) and BAT at 10 min postinjection.

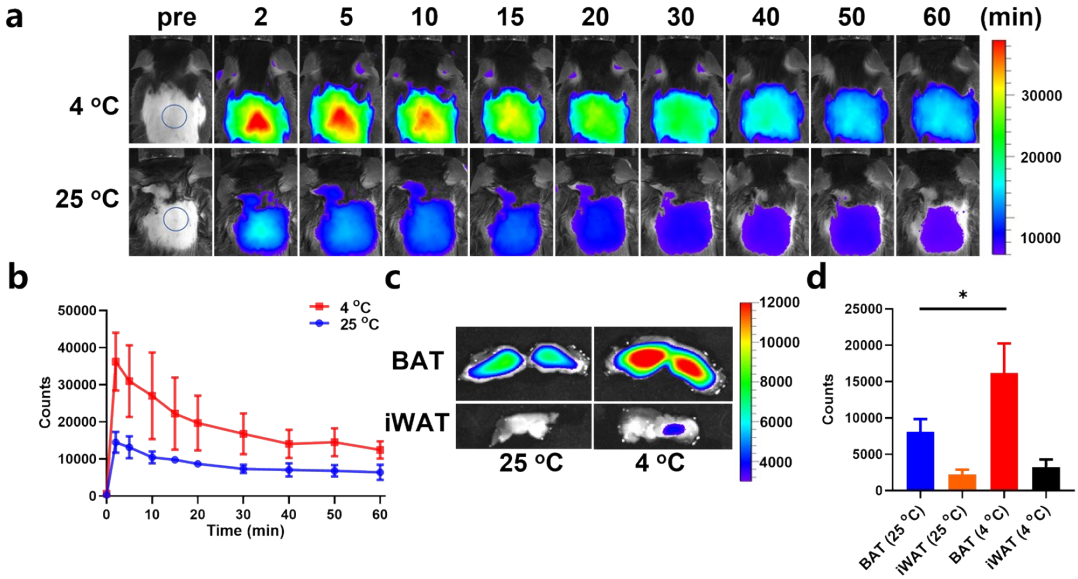

Fig. S9 Evaluation of **HCYBAT-1** for monitoring BAT activation in response to cold exposure. (a) Fluorescence images of cold exposure (4 °C) group and control group (25 °C) (n = 3) at different time points (λ_{ex} = 710 nm, λ_{em} = 810-875 nm). (b) Fluorescent signals of cold exposure (4 °C) and

control mice (25 °C) (n = 3) at different time points (λ_{ex} = 710 nm, λ_{em} = 810-875 nm). *Ex vivo* fluorescence images (c) and intensity analysis (d) of interscapular WAT (iWAT) and BAT at 10 min postinjection.

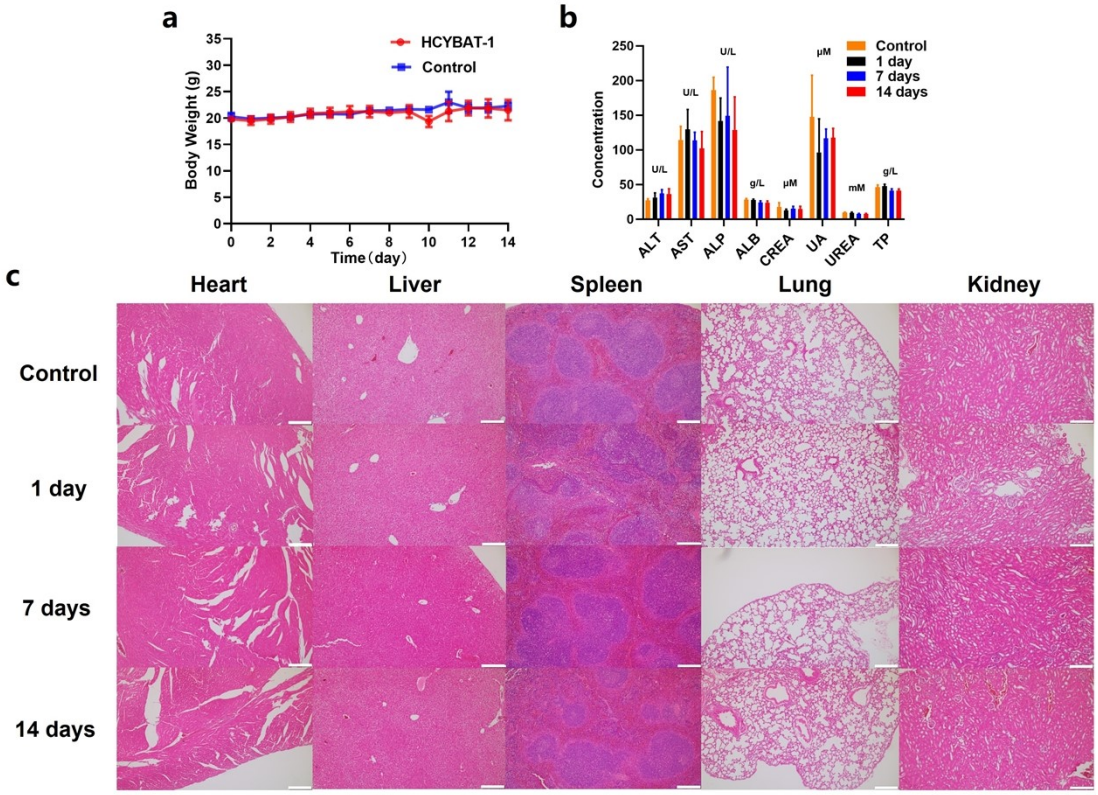

Fig. S10 Biocompatibility of **HCYBAT-1**. (a) Weight recordings within 14 days postinjection of saline solution (control) or **HCYBAT-1** (5.4 μmol/kg, n = 5). (b) Liver and kidney function indicators were achieved at different time points after administration of saline solution (control) or **HCYBAT-1** (5.4 μmol/kg, n = 5). (c) H&E-staining analysis of organs including heart, liver, spleen, lungs, and kidneys on 1 day, 7 days and 14 days after **HCYBAT-1** injection (5.4 μmol/kg, n = 5), scale bar = 200 μm.

^{1}H NMR and ^{13}C NMR spectra

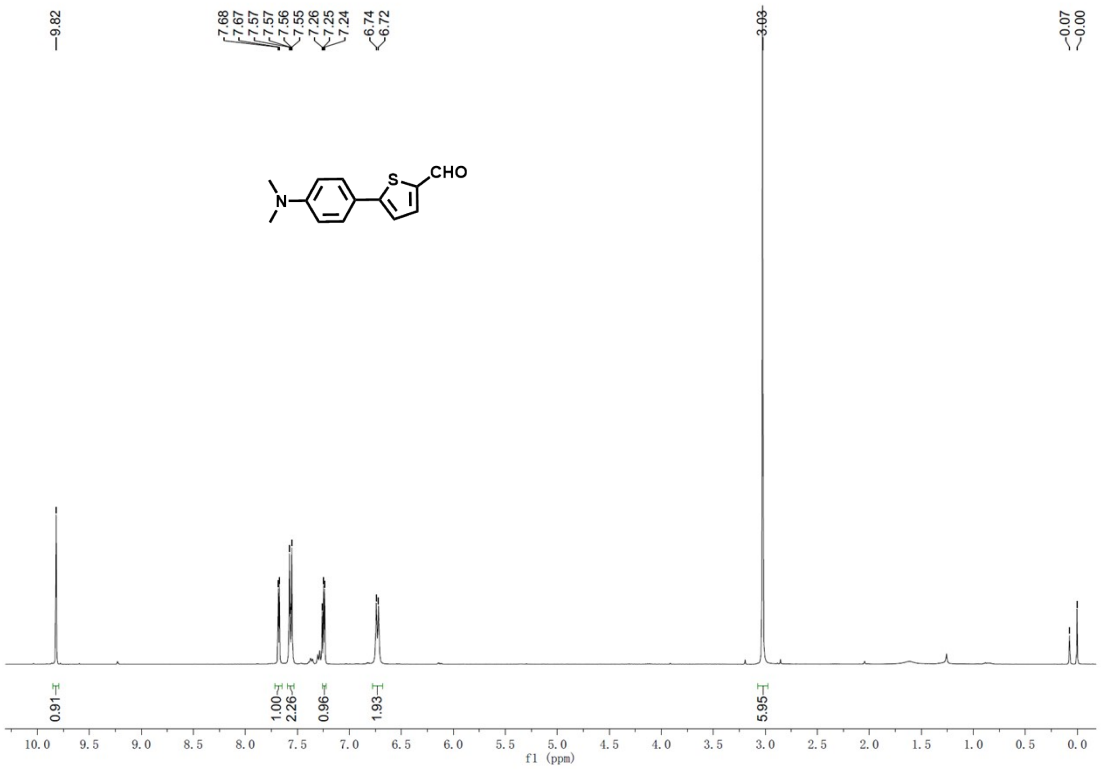

Fig. S11 ^{1}H NMR of compound **3a** (400 MHz, $CDCl_3$).

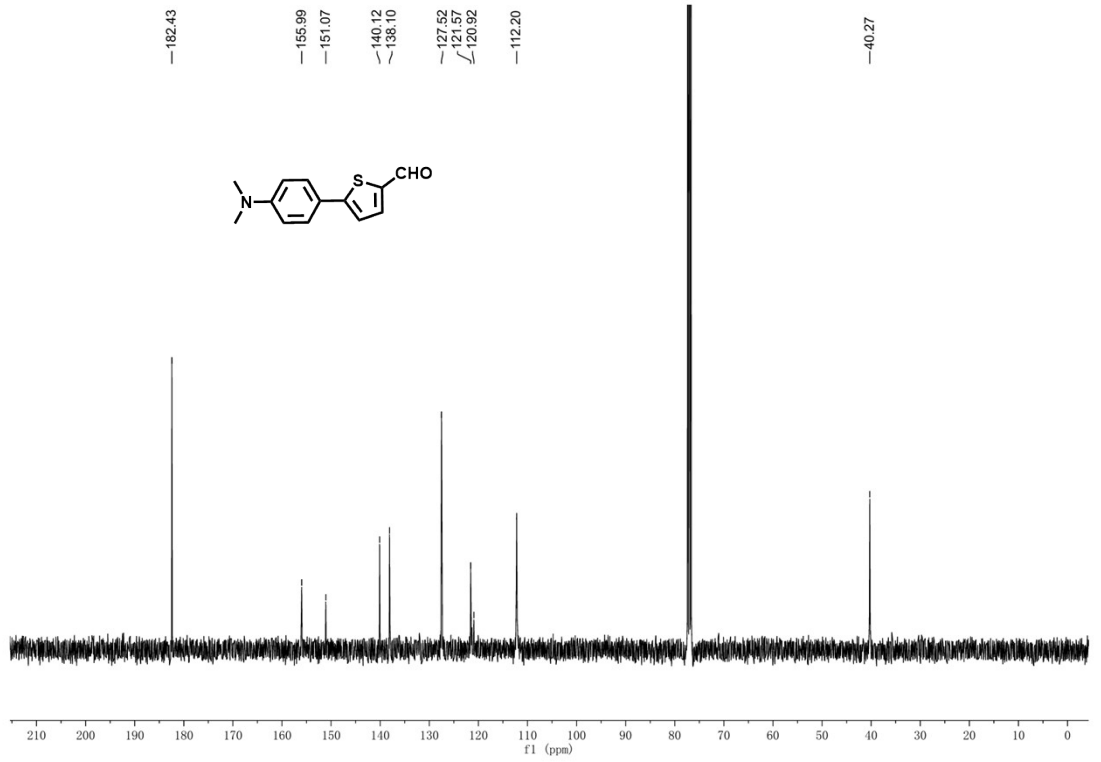

Fig. S12 ^{13}C NMR of compound **3a** (100 MHz, $CDCl_3$).

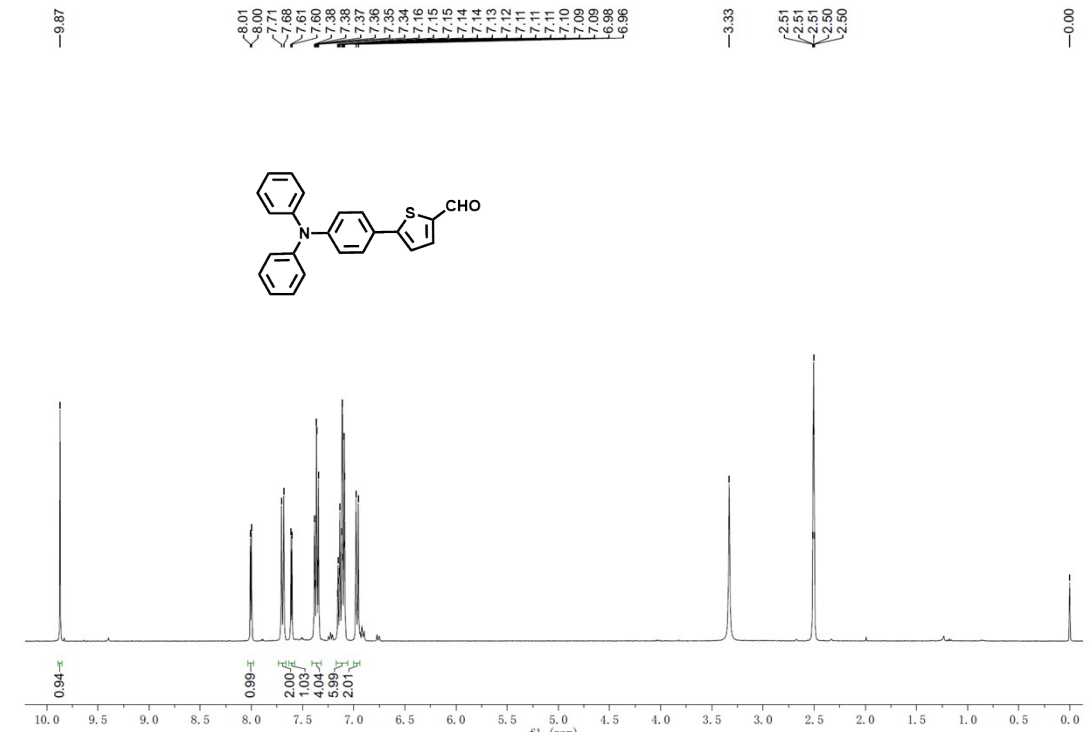

Fig. S13 ^{1}H NMR of compound **3b** (400 MHz, $CDCl_3$).

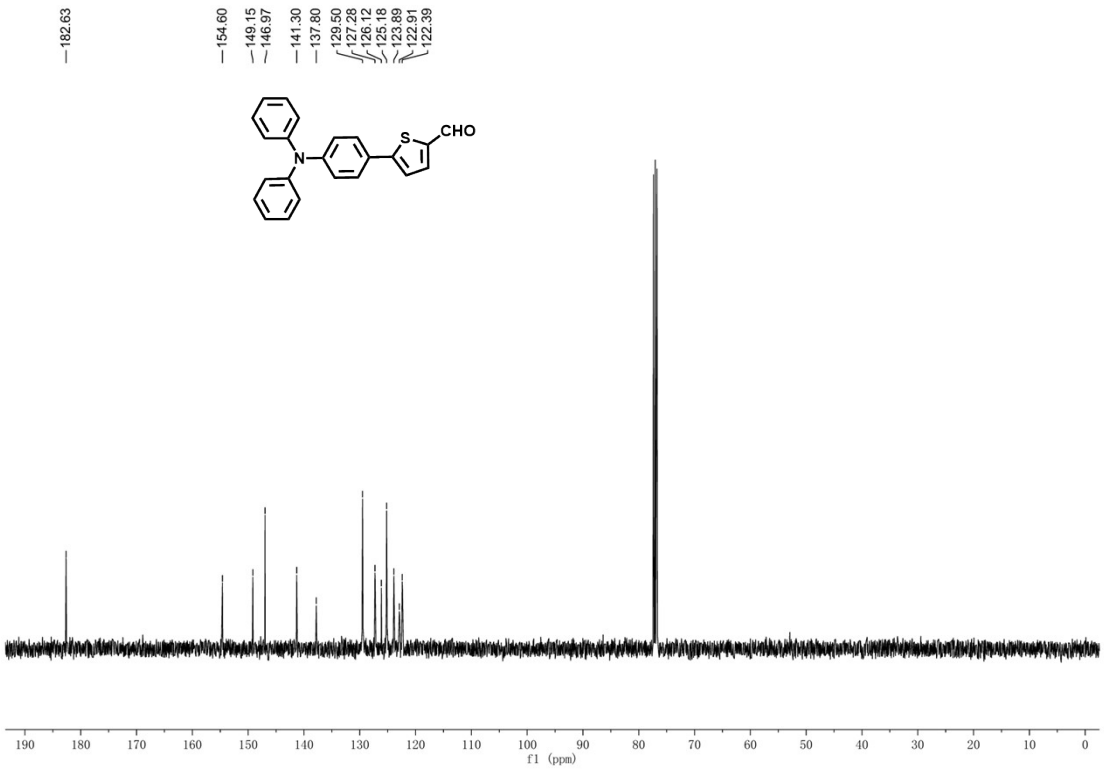

Fig. S14 ^{13}C NMR of compound **3b** (100 MHz, $CDCl_3$).

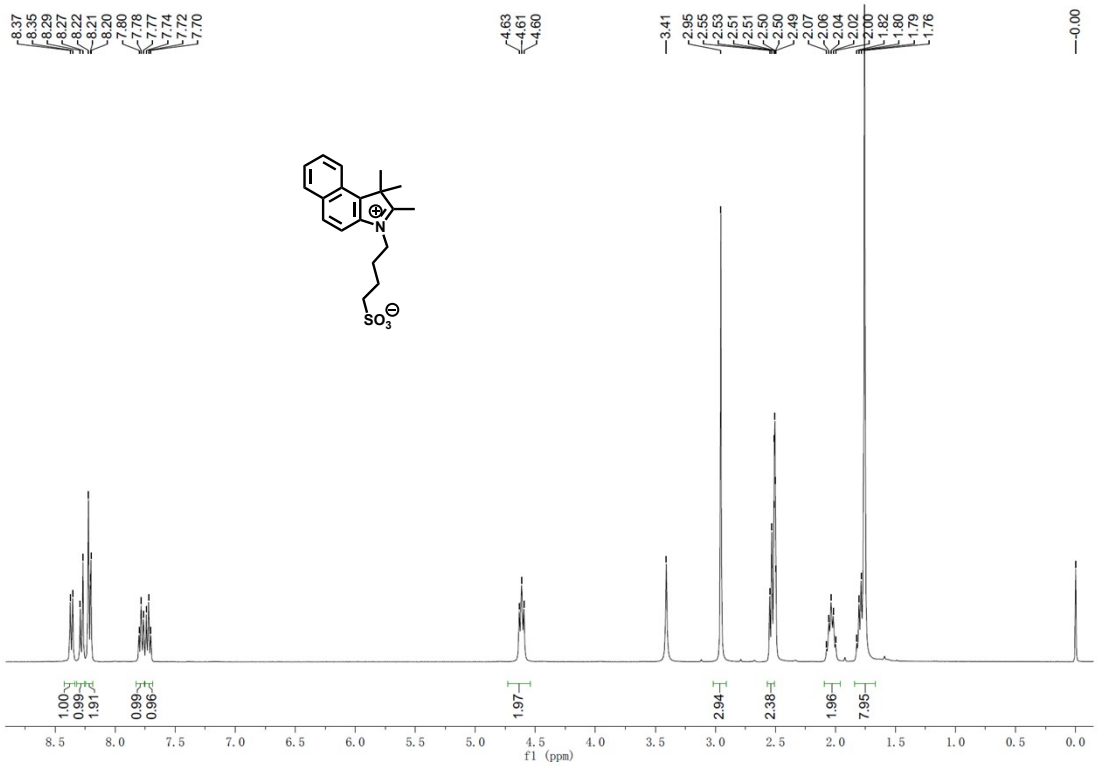

Fig. S15 [1]H NMR of compound **5a** (400 MHz, DMSO-d_6).

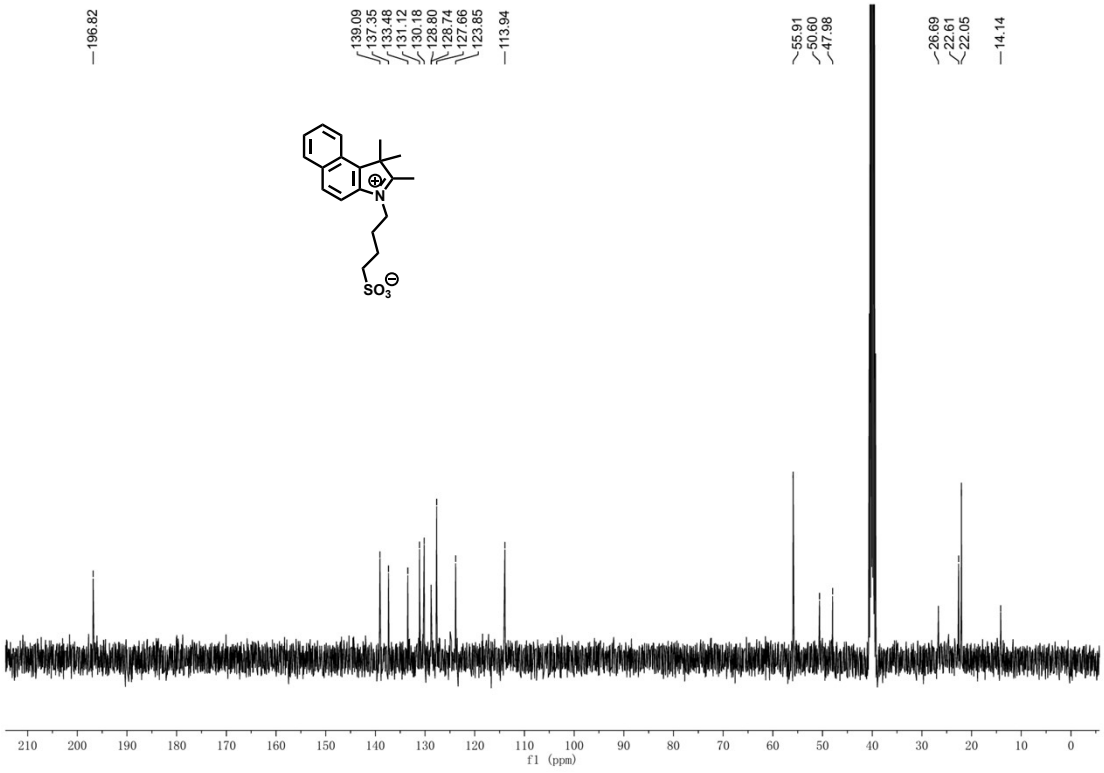

Fig. S16 [13]C NMR of compound **5a** (100 MHz, DMSO-d_6).

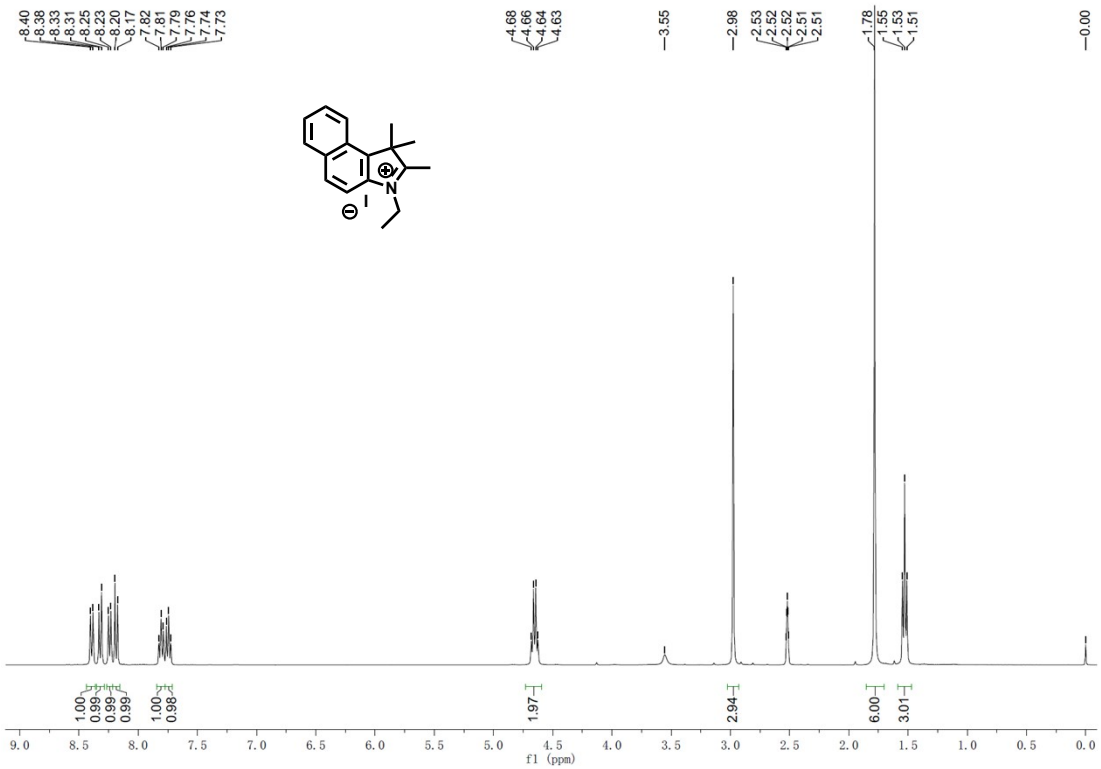

Fig. S17 ^{1}H NMR of compound **5b** (400 MHz, DMSO-d_6).

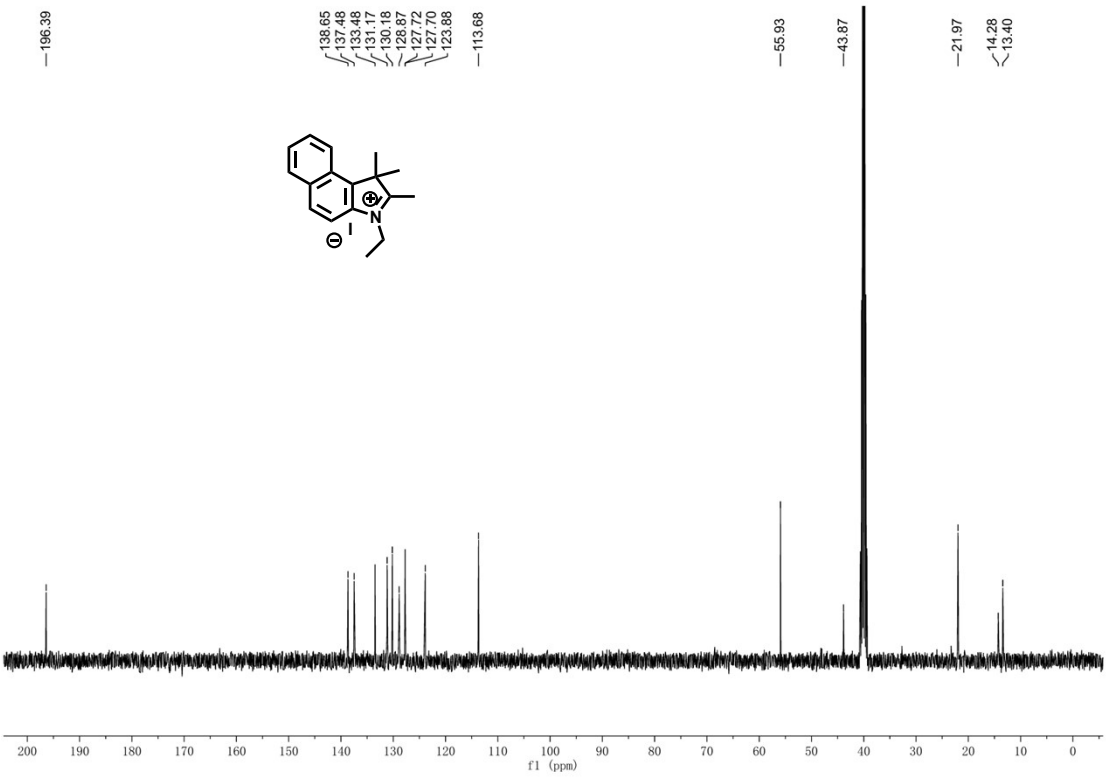

Fig. S18 ^{13}C NMR of compound **5b** (100 MHz, DMSO-d_6).

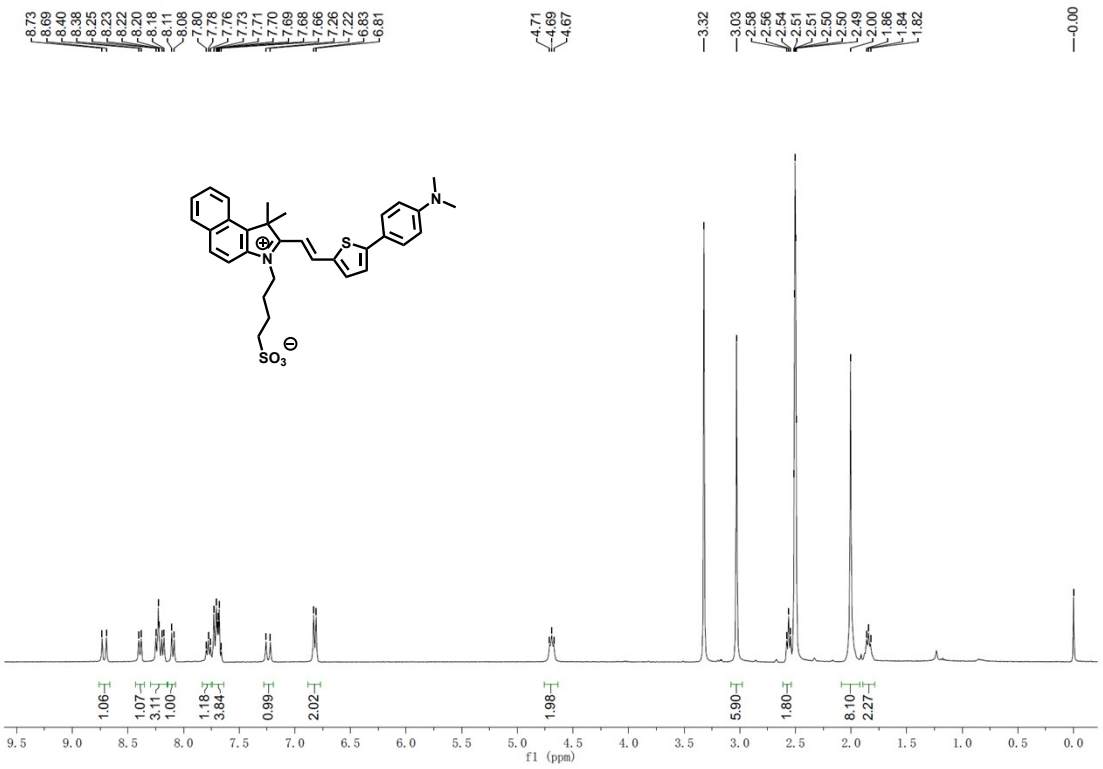

Fig. S19 ^{1}H NMR of **HCYBAT-1** (400 MHz, DMSO-d_6).

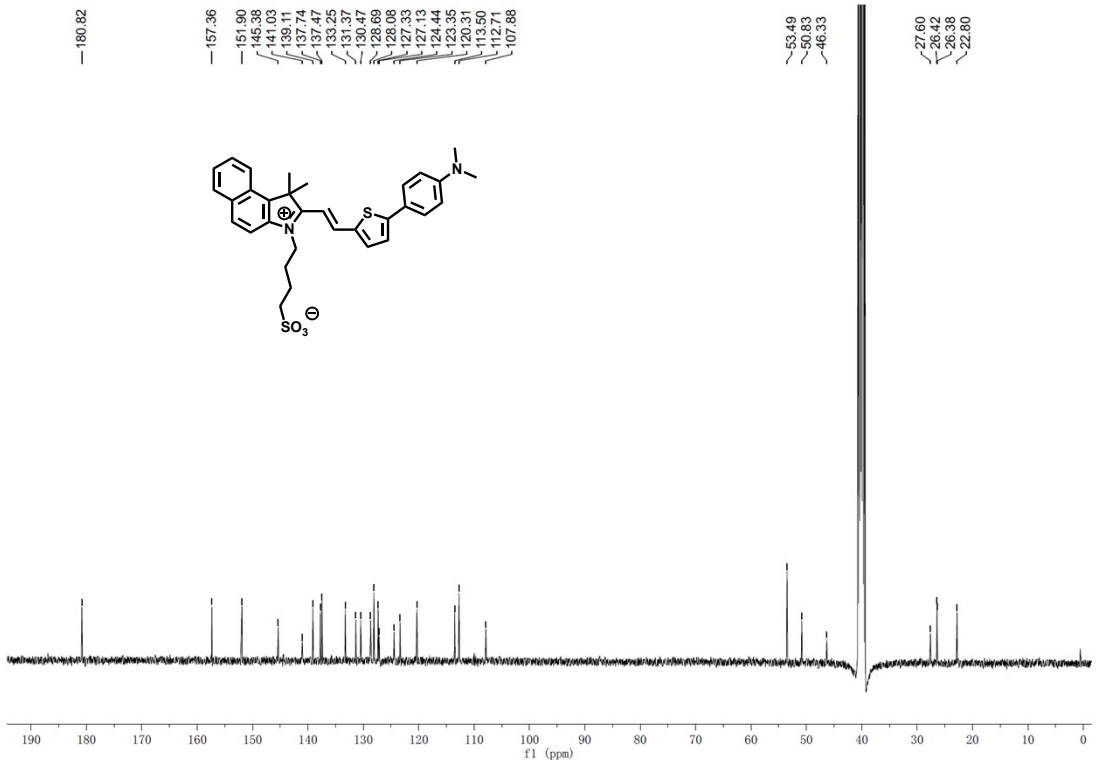

Fig. S20 ^{13}C NMR of **HCYBAT-1** (100 MHz, DMSO-d_6).

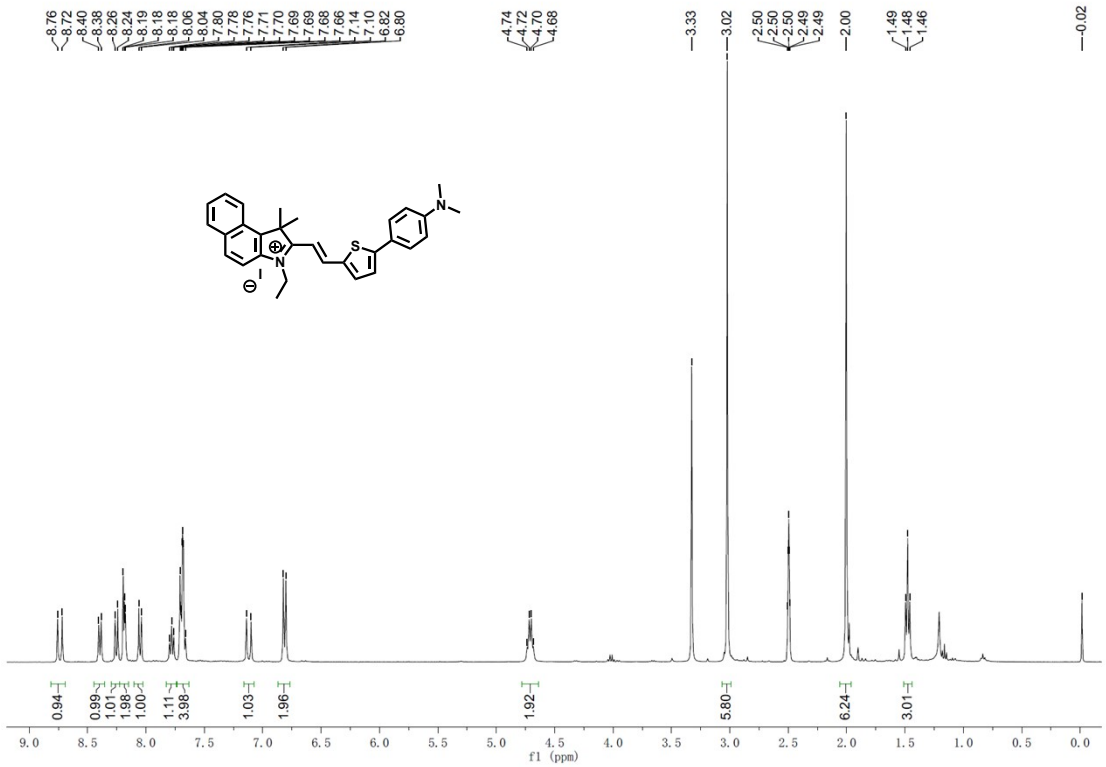

Fig. S21 ^{1}H NMR of **HCYBAT-2** (400 MHz, DMSO-d_6).

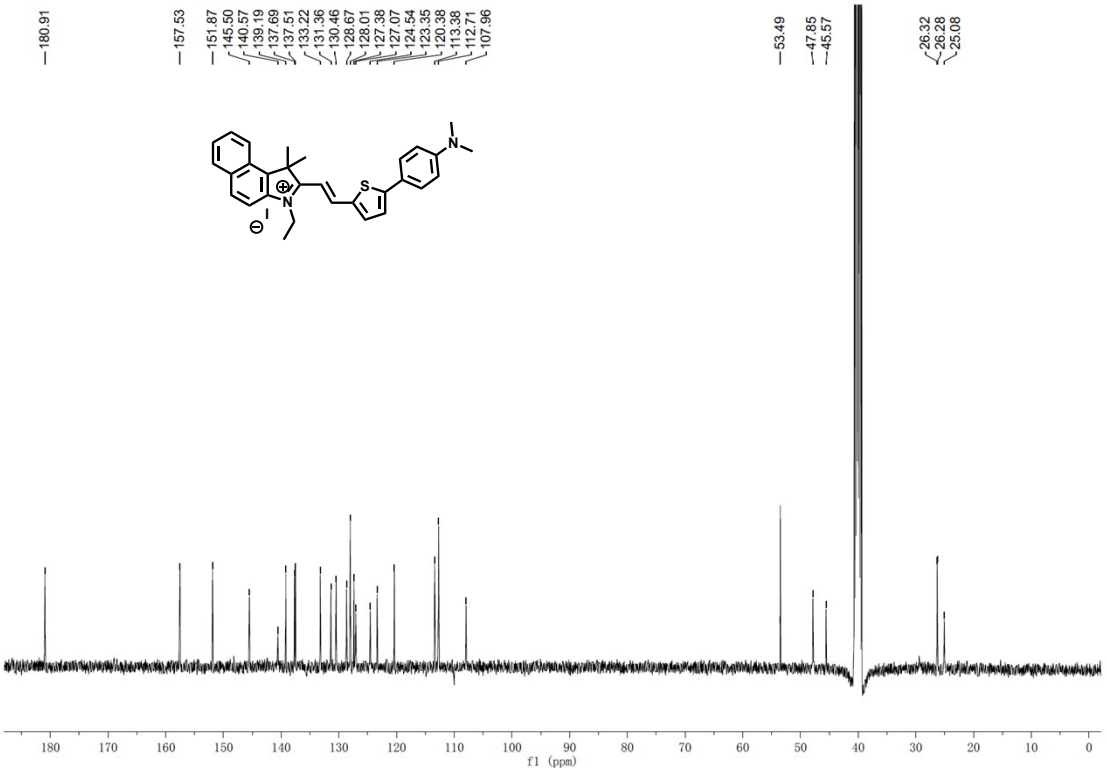

Fig. S22 ^{13}C NMR of **HCYBAT-2** (100 MHz, DMSO-d_6).

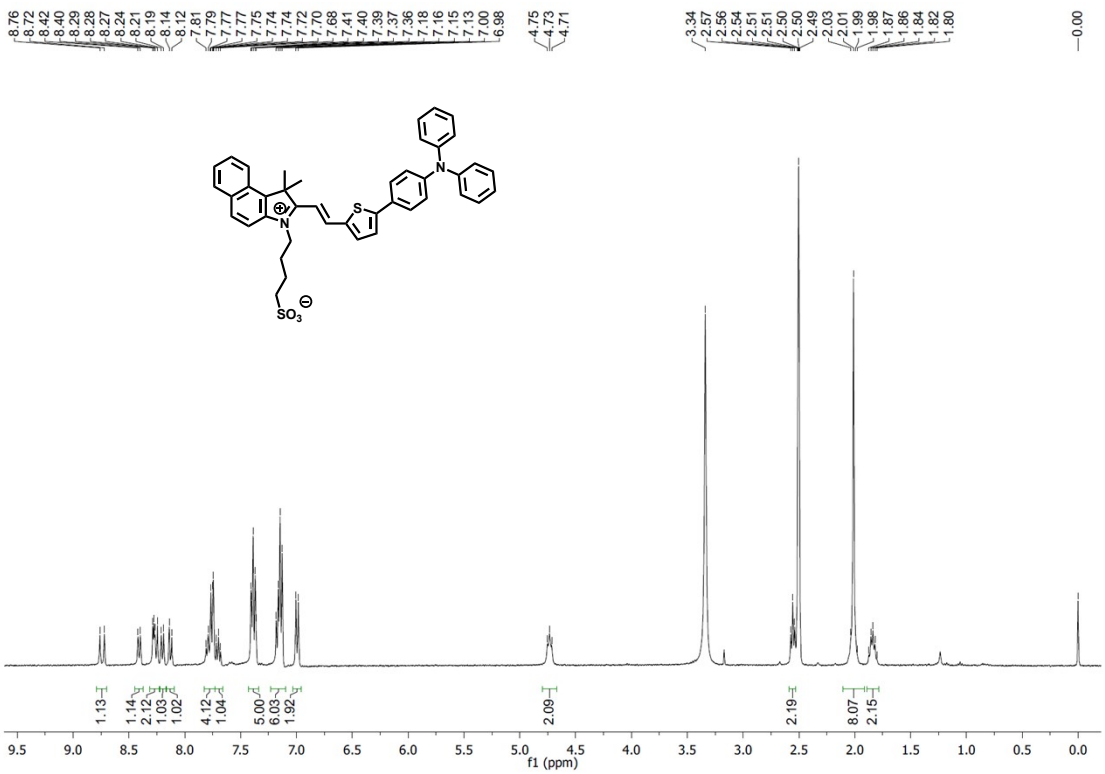

Fig. S23 ^{1}H NMR of **HCYBAT-3** (400 MHz, DMSO-d_6).

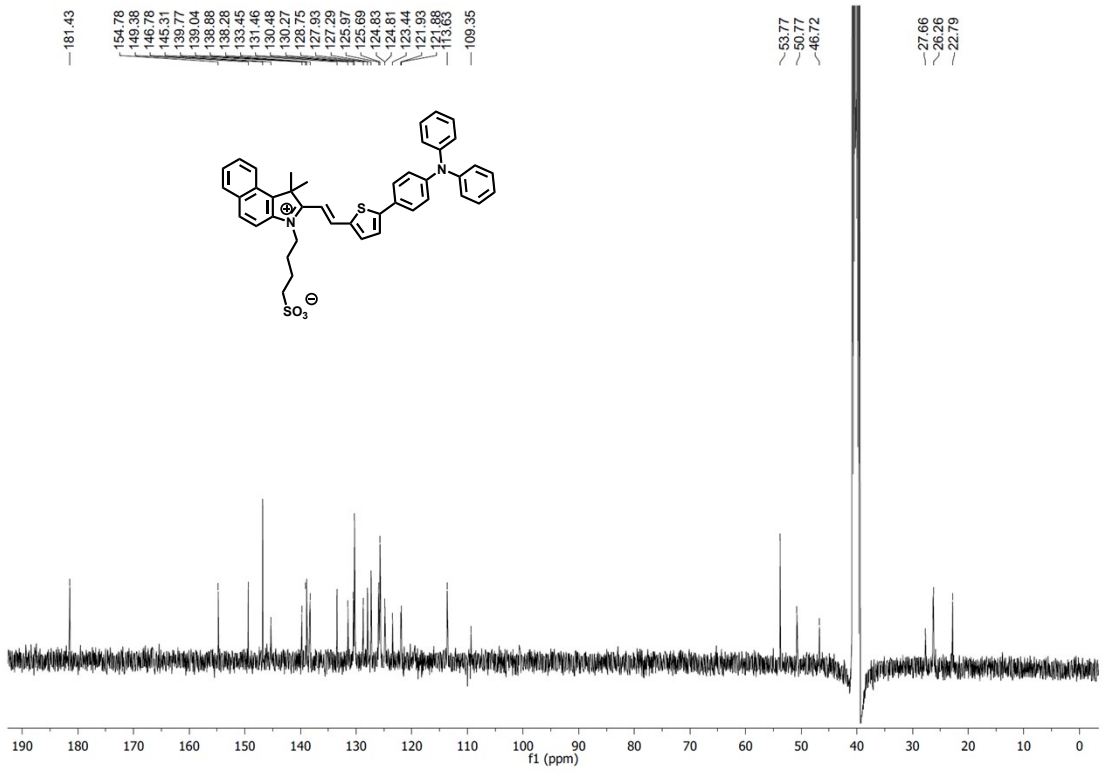

Fig. S24 ^{13}C NMR of **HCYBAT-3** (100 MHz, DMSO-d_6).

HRMS spectra

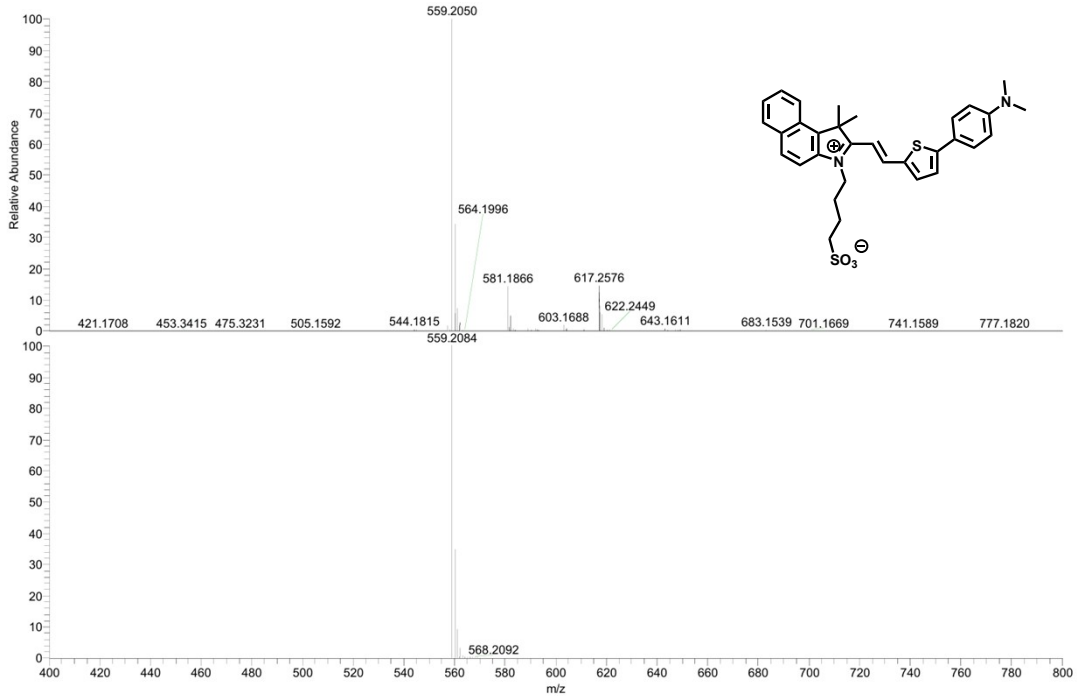

Fig. S25 HRMS spectrum of **HCYBAT-1**.

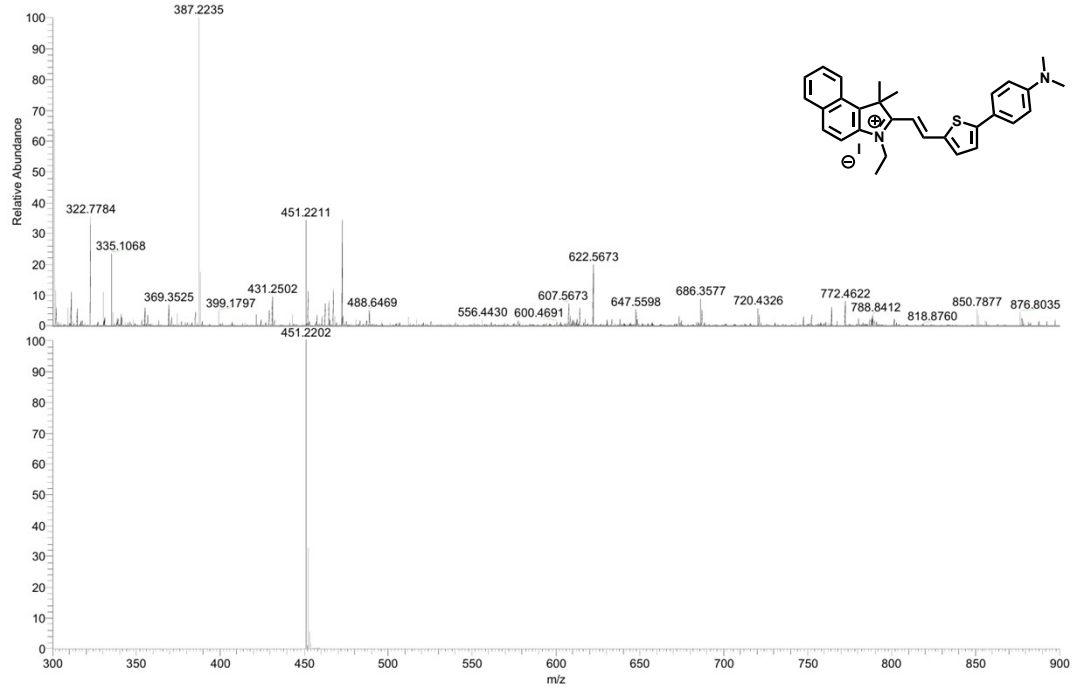

Fig. S26 HRMS spectrum of **HCYBAT-2**.

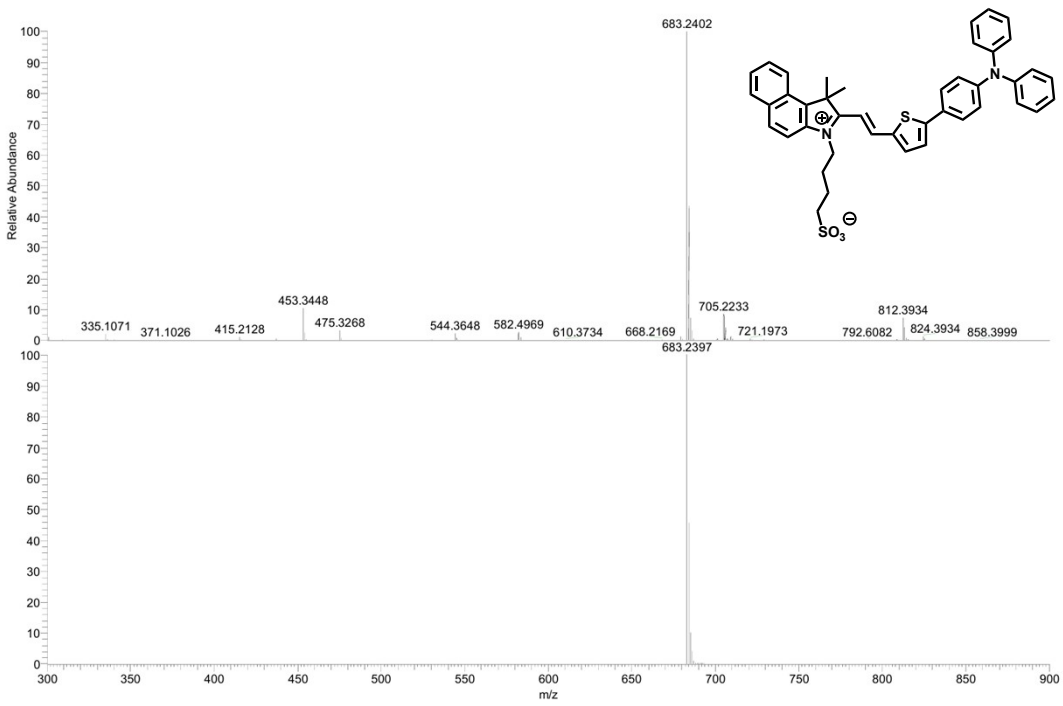

Fig. S27 HRMS spectrum of **HCYBAT-3**.

HPLC spectra

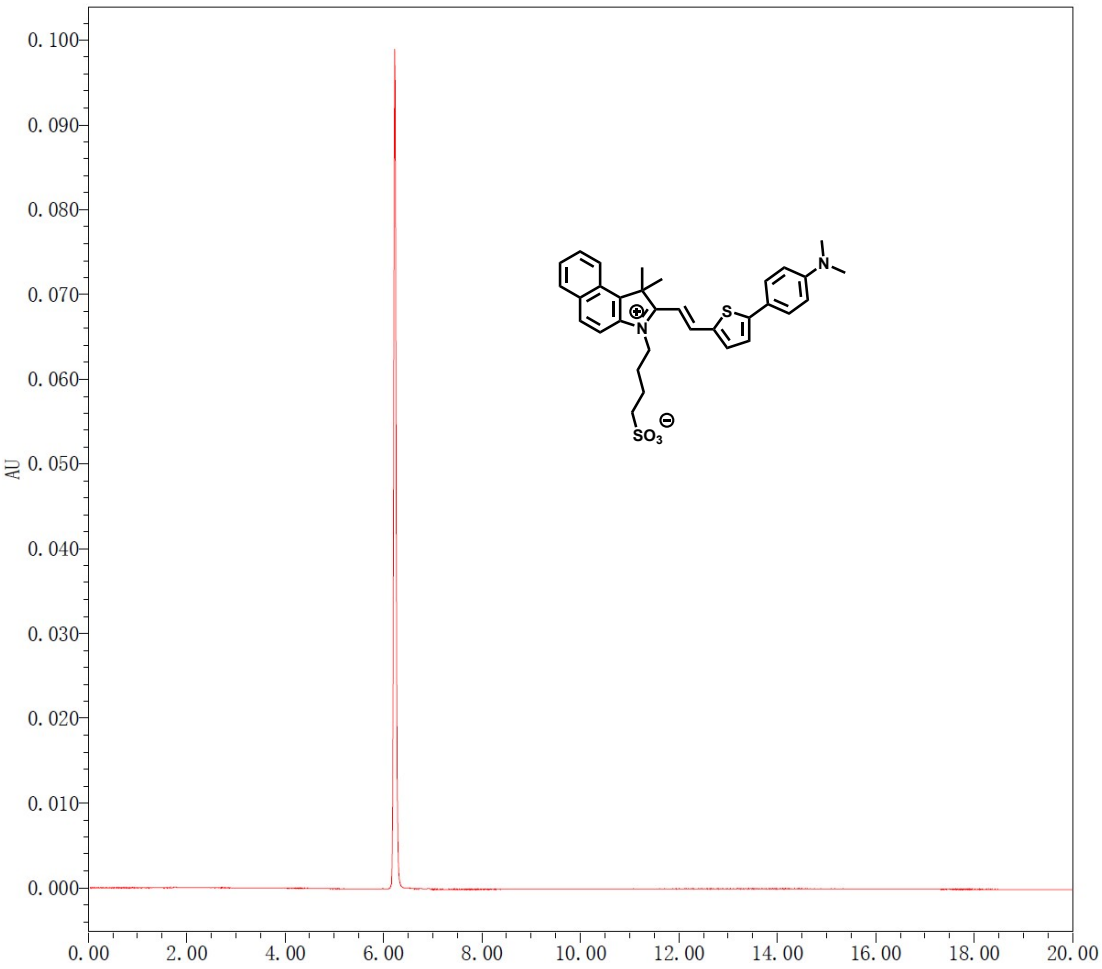

Fig. S28 Analytical HPLC spectrum of **HCYBAT-1**.

HPLC parameters

	MeOH (0.1% TFA)	H_2O (0.1% TFA)
0 min	30%	70%
2 min	50%	50%
4 min	100%	0%

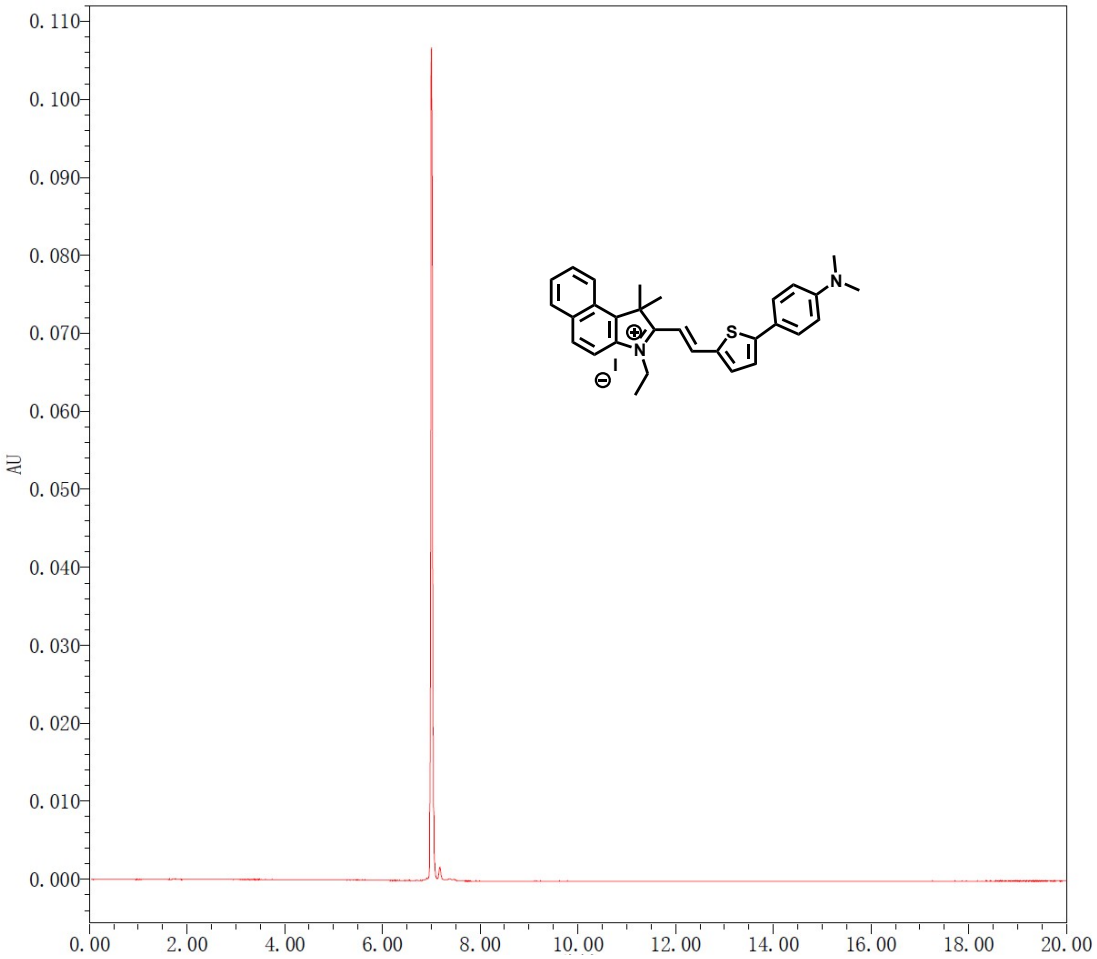

Fig. S29 Analytical HPLC spectrum of **HCYBAT-2**.

HPLC parameters

	MeOH (0.1% TFA)	H_2O (0.1% TFA)
0 min	30%	70%
3 min	50%	50%
5 min	100%	0%

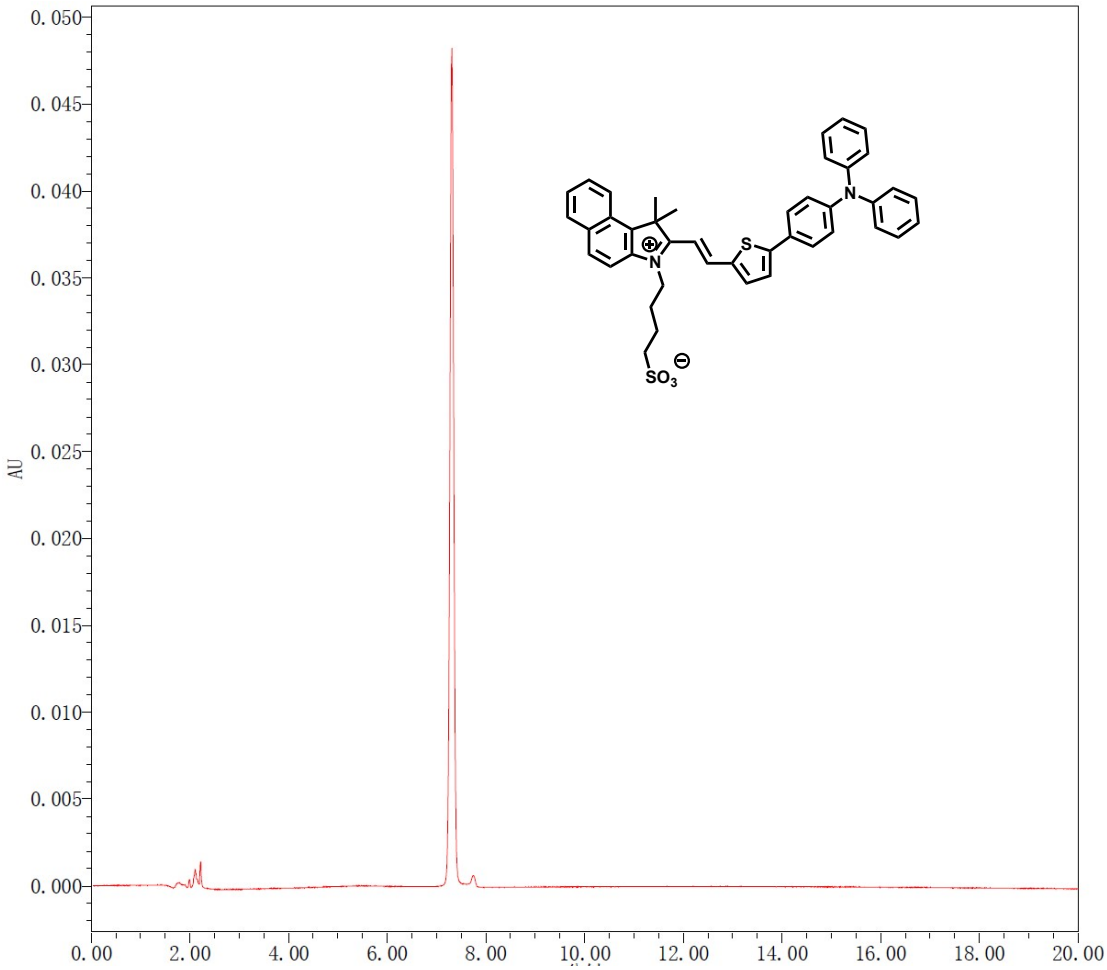

Fig. S30 Analytical HPLC spectrum of **HCYBAT-3**.

HPLC parameters

	MeOH (0.1% TFA)	H_2O (0.1% TFA)
0 min	30%	70%
3 min	50%	50%
5 min	100%	0%

12 References

1 J. Shao, S. Ji, X. Li, J. Zhao, F. Zhou and H. Guo, *Eur. J. Org. Chem.*, 2011, **2011**, 6100-6109.

2 J. Wan, Y. Li, K. Jin, J. Guo, J. Xu and C. Wang, *ACS Appl. Mater. Interfaces*, 2020, **12**, 23717-23725.

3 J. Hong, J. Zhang, Q. Li and G. Feng, *Anal. Chem.*, 2023, **95**, 2671-2679.

4 J. Liu, W. Zhang, C. Zhou, M. Li, X. Wang, W. Zhang, Z. Liu, L. Wu, T. D. James, P. Li and B. Tang, *J. Am. Chem. Soc.*, 2022, **144**, 13586-13599.

5 L. Lai, R. Wang and Y. Tang, *Acta Phys. Chim. Sin.*, 1994, **10**, 963-965.